Board-To-Board Optical Interconnects Utilizing Molded Embedded 45 Degree Mirrors and Print-on-Demand Micro-lenses as Proximity Vertical Coupler

Xiaohui Lin[a], Amir Hosseini[b], Xinyuan Dou[a], Harish Subbaraman[b], and Ray T. Chen[1,*], Fellow, IEEE

[a] Department of Electrical and Computer Engineering, the University of Texas at Austin, Austin, TX, 78758, USA

[b] Omega Optics, Inc., 10306 Sausalito Dr, Austin, TX 78759, USA

ABSTRACT

We demonstrate board-to-board optical communication utilizing 45 degree mirrors and print-on-demand micro-lenses as surface-normal coupler. The presented system which includes polymer waveguides, embedded 45 degree mirrors and micro-lenses, realizes back-to-back optical interconnects between two boards. The waveguide and mirrors are fabricated using molding method using a low-cost electroplated nickel mold. Micro-lenses (80 μm in diameter) are fabricated using a material inkjet-printer, on top of the 45 degree mirrors. Experimental results show that each 45 degree mirror contributes about 1.88 dB loss (65% coupling efficiency) to the total optical loss. When propagating in free space without a lens, a 2 mm separation between boards results in a 9.9 dB loss, which is reduced to 7.5 dB when a micro-lens is inserted in the path. High speed data transmission test is performed at various separations. At a separation of 1mm, the system can provide 10Gbps error free transmission. At 2mm separation, the maximum error free data rate was measured to be 3.5Gbps and 7.5Gbps, with and without the micro-lens, respectively. Printing the micro-lenses on both the input 45 degree mirror and the photodiode or the receiving 45 degree mirror in a confocal setup will significantly reduce the free-space propagation loss. To the best of our knowledge, this is the first report of free-space coupling between waveguides on separate boards.

Keywords: board-to-board optical interconnects, molding, embedded 45 degree mirror, inkjet-printed micro-lenses

1. INTRODUCTION

The development of optical components and system solutions is enabling high bandwidth communication in chip-to-chip [1, 2], intra-board [3, 4], board-to-board [5-7], card-to-backplane [8, 9] and rack-to-rack links [10, 11]. Optical interconnects are proving to be a superior alternative to their electrical counterparts, in terms of cost, power, and bandwidth [12, 13].

Board-to-Board parallel data transmission through optical means is attracting increasing attention across the research community. Free-space optical interconnects between VCSELs and photodetectors (PDs) placed on separate boards have been demonstrated in which fixed integrated micro-lens arrays [14, 15] or MEMS controlled lens arrays were used to lower optical loss by reducing the beam divergence [16-18]. In this paper, we describe a novel concept of optical interconnects using a back-to-back layout. Free space surface normal coupling is realized by a customized proximity coupler consisting of 45 degree reflective mirrors and ink-jet printed micro lenses. Figure 1 illustrates this idea. It can be seen from the figure that the electrical layer and optical layer are located at different sides of the board, which shortens the distance between two optical layers. Within a few millimeter separation, free-space optical interconnects can be realized. Also, one board can communicate with several boards by placing the coupler at different locations. Inkjet-printed micro-lenses are placed on the top of the 45 degree mirrors, which significantly decrease the divergence and increase the quality of collimation of the vertical beam. The VCSELs and PDs in the optical layer can be controlled by signals transmitted through vias from the electric layer. After prototype fabrication, the optical transmission quality in

* Ray T. Chen: chen@ece.utexas.edu

Optoelectronic Interconnects XIII, edited by Alexei L. Glebov, Ray T. Chen, Proc. of SPIE Vol. 8630, 86300A · © 2013 SPIE · CCC code: 0277-786/13/$18 · doi: 10.1117/12.2009447

setups using two mirrors and four mirrors in the optical path are evaluated. Losses as a function of different board-to-board separations are also measured. In order to investigate the effects of inkjet-printed micro-lens, insertion losses with and without the micro-lenses are compared.

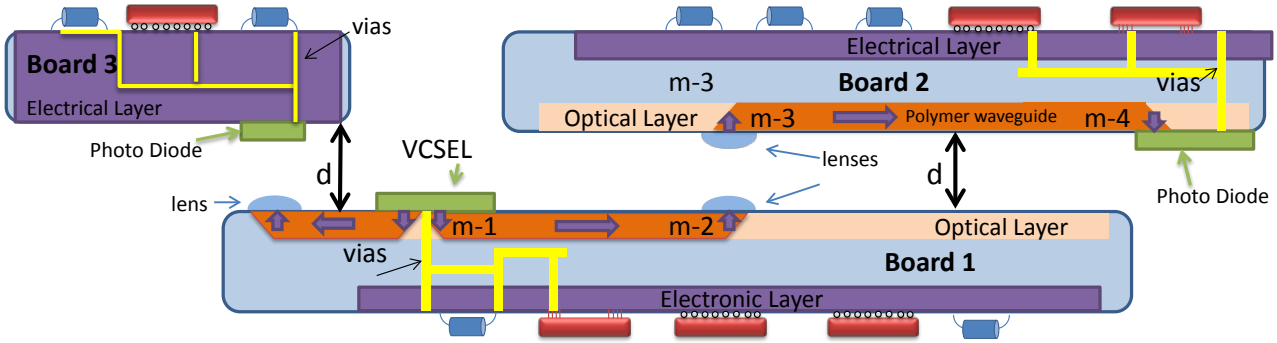

Figure 1 Inter- and intra-board optical interconnects with polymer waveguides and 45 degree couplers with ink-jet printed micro-lenses

2. REALIZATION OF PROXIMITY COUPLER

The proximity coupler is formed by a 45 degree reflective mirror and ink-jet printed micro-lenses. 45 degree mirror based coupling method to integrate VCSELs and PDs in one of PCB board layers has been previously demonstrated[19, 20]. Coupling efficiency varies from around 3dB [21, 22], 2.3dB [23] down to 1.74dB[24] and 0.5dB[25] per mirror, based on different fabrication methods. To maximize the coupling efficiency, there are a few methods utilizing precisely positioned external coupling modules [7] or external lenses [26, 27]. These are feasible methods, but such external components usually have large footprints and are not suitable for system integration.

Different from all above work, we fabricate embedded total internal reflection (TIR) mirrors in a single-step molding process using nickel mold. A similar process has been reported by Wang [28], but using silicon mold. Nickel molds are advantageous over silicon molds because they can be formed by an electroplating method to reach 50μm height. Etching silicon to the same depth with a vertical sidewall is rather challenging. For the micro lenses used for improving coupling efficiency, we utilized an ink-jet printing method which directly forms the lenses at desired locations without any complicated process and increase in system footprint. The embedded mirrors together with the inkjet-printed micro-lenses on top serve as proximity couplers for board-to-board free-space optical interconnects between two molded waveguides on separate boards. The molding and ink-jet printing methods are described below.

2.1 Polymer waveguide with 45 degree reflective mirror

We fabricate polymer waveguides with embedded 45 degree mirrors using molding method. The fabrication is composed of four main steps as illustrated in Figure 2: (a) SU8 pre-mold fabrication, (b) nickel metal mold by electroplating, (c) molding process, and (d) waveguide fabrication. SEM pictures (for steps a, b and c) and microscopic pictures (for step d) are also shown.

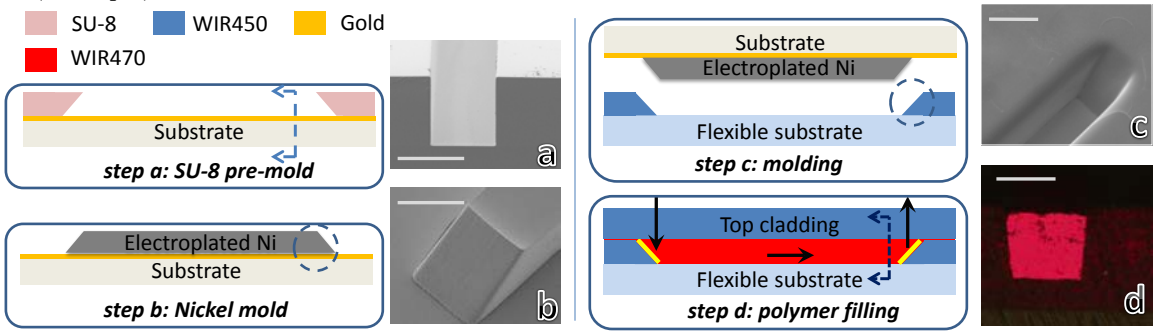

Figure 2 Fabrication process for molded channel waveguide with 45 degree embedded mirror coupler. The scale bar represents 50μm length.

The 1st step (step a) involves making an SU8 pre-mold with 45 degree mirrors on both sides. The pre-mold is used as a template for the nickel hard mold fabrication and its quality is of great importance for all the following steps. First, a thin layer of 5 nm/50 nm Ti/Au layer is coated by evaporation, and it serves as a seed layer for electroplating nickel performed in step b, as shown in Fig. 2. Following this, a 50 µm thick SU-8 layer is deposited on the seed layer and patterned by immersed tilted exposure to form the 45° slants. The detailed description can be found in [29].

Nickel hard mold is achieved by electroplating nickel into the SU8 pattern. Compared to the evaporation/lift-off methods, electroplating is featured by its high deposition rate, and makes its ability to deposit 50µm in around 7 hours. We use a commercially available Ni electroplating kit from Caswell Inc. The pre-buried Ti/Au layer serves as the seed layer for electroplating. In order to achieve the required adhesion between the seed layer and the nickel layer, the electro-plating current density is initially kept low at 1 mA/cm^2 for 5 minutes. Then, the current density is raised to 10 mA/cm^2 to achieve a deposition rate of 120 nm/min. At the end, a low current density 1 mA/cm^2 is applied for 5 minutes to improve film quality. Next, the SU-8 resist is removed by Remover PG to release the nickel mold. The cross linked SU-8 resist is hard to be removed by any solvent therefore, it is important to have a release layer underneath the SU-8 layer, for example Omnicoat, to help peel off the cross linked SU-8 completely.

The imprinting process is performed to the bottom cladding material WIR30-450 (n=1.45@850 nm). The cladding material is firstly spin-coated onto TEONEX (from DuPont Teijin Films Inc.) substrate with an adhesion promoter in-between, followed by Ultraviolet (UV) light curing. To ensure that the mold can be effectively detached from the substrate during the molding process, AZ5209 photo resist is spin-coated on nickel hard mold as the release layer. At the same time, this release layer also helps reducing the surface roughness of mold. Atomic force microscopy (AFM) reveals that the surface roughness of the mold is reduced from 70nm to 2~3nm by resist coating. After molding, the polymer is UV cured. Next, the de-molding process is completed in acetone, which dissolves the photo resist in-between the mold and device. The molded surface roughness is less than 5nm as reported before [30].

The molded bottom cladding layer is mounted on the evaporation chamber and 200 nm of gold is coated onto the slope region using a shadow mask. Gold coating helps in enhancing the reflectivity of the mirror, which in turn increases the coupling efficiency. The imprinted trenches are filled with the core material WIR30-470 (n=1.47@850 nm). Next, the core material is UV cured for 12 mins, followed by coating of the top cladding material. Then the substrate can be attached to a silicon wafer or PCB board for further processes.

2.2 Micro-Lens fabrication process

Due to the fact that the optical signal receiving area is about the same size as the output end, the divergence of light during transmission makes the collected energy at the receiving side very limited. Inserting a micro-lens in the optical path helps in reducing the divergence angle of output light from the 45 degree mirrors so that more signal can be collected. Conventionally, the micro-lenses have been fabricated based on photoresist melt-and-reflow technique [27, 31]. In this work, the micro-lenses are directly ink-jet printed over the 45 degree mirrors, similar to the method reported in [32]. In our experiment, we use diluted glycerol (glycerol:BPS=3:7 by volume) to form the micro-lens with index of 1.46556 at 850 nm wavelength. The ink-jet printer used in this work is a Fujifilm Dimatix Materials Printer (DMP-2800) which utilizes a piezoelectric printing cartridge (DMC-11610) to dispense a nominal volume of 10pL each cycle for one nozzle. By specifying the desired printing position, the micro-lens can be placed above the targeted 45 mirror coupler with good accuracy. Figure 3(a) and Figure 3(b) show the top view of the mirror before and after inkjet-printing the micro-lens. A contact angle goniometer is used to take the profile of the droplet, as shown in Figure 3(c).

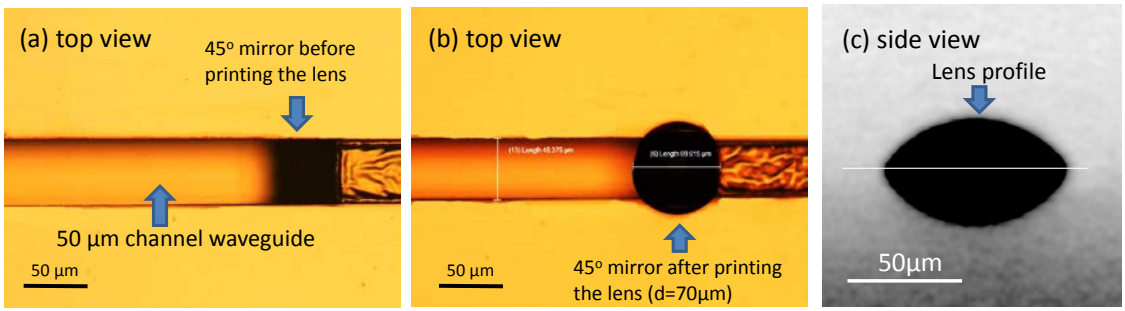

Figure 3(a) top view of embedded mirror before printing micro-lens (b) top view of embedded mirror after printing micro-lens with d=70µm. (c) the lens profile taken by contact angle goniometer.

The lens profile, which determines the focal length, can be adjusted by varying the viscosity of the printed material or surface properties of the substrate. Also, UV curable material can be adopted and cured to permanently fix the shape of the micro-lens [32]. Different focal lengths have been reported, for example, 48 µm [33], 55-153 µm [34], a few hundred microns [16, 35-37], or in millimeter range [5], with different materials and lens profiles. Currently, the printed droplets in this work are 70µm in diameter with 100-150 µm focal lengths estimated using the relations in [38]. The focal length can be controlled by the combination of surface properties, material viscosity and ink volumes. We are still investigating the effects of refractive index, size, curvature and contact angle of the inkjet-printed lenses. By fine tuning the lens profile, optimized focal length can be achieved to make sure that the light collected at the receiving end is maximized.

3. OPTICAL LOSS EVALUATION

3.1 Testing setup

Schematics of the board-to-board interconnect setups using the 45 degree mirrors are shown in Figure 4. In the first experimental setup, shown in Figure 4(a), a VCSEL (850 nm) is coupled to a 4.5 cm polymer intra-board channel waveguide through a 45 degree mirror. Another 45 degree mirror is used to couple light out of the waveguide. A PD placed on a separate board converts the optical signal into an electrical signal. In the second experiment setup, shown in Figure 4(b), two identical waveguides (each 4.5 cm long) on separate boards with adjustable separation *d* are used to couple light from a VCSEL on one board to a PD on the other board through using four 45 degree mirrors. We also compare cases with and without micro-lenses.

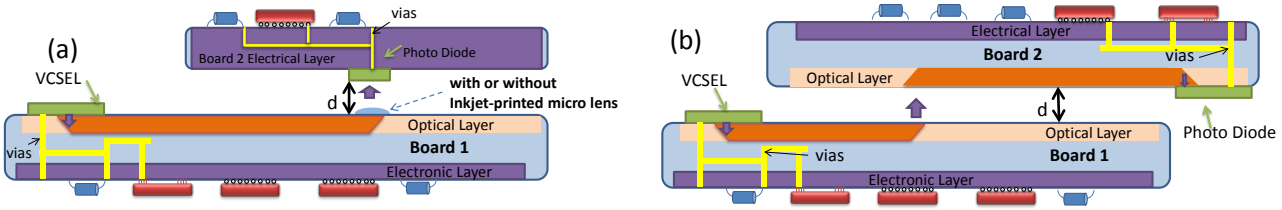

Figure 4 Board-to-board experimental setup showing, (a) one waveguide with two 45 degree mirrors, (b) two waveguides with four 45 degree mirrors. Visible spots show the output after 2 mirrors and 4 mirrors. They are used for pre-alignment of two boards (632 nm visible laser as input, only for pre-alignment)

3.2 Optical loss evaluation

Figure 5 shows the variation of the measured optical power from the PD for 850nm wavelength as a function of the separation between the boards. The total optical loss is composed of the free space propagation loss and the insertion loss, which is determined by the coupling method and the propagation loss of the polymer waveguide. It can be seen from Figure 5(a), for d=0 (where the free space propagation loss is zero), that the measured insertion loss (without a micro-lens) is 4.586 dB. We have measured the propagation loss and scattering loss for the WIR polymer waveguides fabricated using molding method, and the loss was found to be 0.18dB/cm[29]. Therefore, each 45 mirror coupler contributes 1.888 dB loss to the optical path total loss, which corresponds to 64.86% coupling efficiency. Due to the divergence of the light coupled out of the waveguide by the 45 degree mirror, the total optical loss increases with increasing d. The divergence angle of the out-coupled beam can be reduced when a micro-lens is inserted in the optical path. Figure 5 shows 1.5 dB improvement at shorter separation (1-2 mm) and 3.7 dB improvement at larger separation (4 mm).

Furthermore, the free space coupling loss due to the beam divergence can also be extracted from the total insertion loss, as shown in Figure 5(b). For comparison, the loss versus distance result from a previous report that utilized relatively larger lenses (240 um in diameter) mounted on both the output and input ends [5] is also plotted. The minimum loss on the results from [5] occurs at a free space propagation distance corresponding to the confocal length of the two lens system.

For the second experiment, the total insertion loss in 12 dB at d=1 mm. The difference between the total insertion loss values from the two experiments remains about 4.4~4.8 dB (average=4.528 dB) regardless of d as long as it is within 3mm. By subtracting the propagation loss (0.18 dB/cm) from all the waveguides in the second experiment, we estimate the coupling efficiency of each of the extra 45 degree mirrors in the second experiment to be 65.22%, which is very similar to the mirror coupling efficiency of the 1st board. Since the two channels are molded with the same nickel hard mold, it further confirms the process stability for such molding fabrication process.

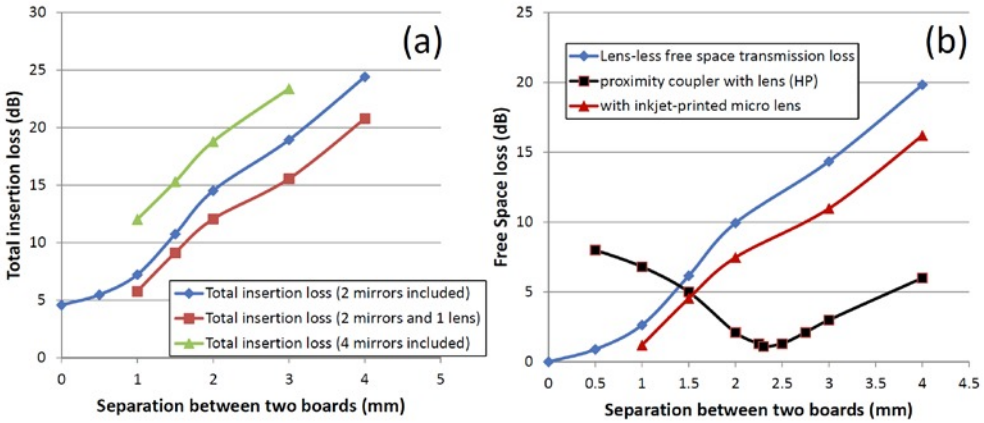

Figure 5(a) Total insertion loss with the separation between two boards, when 2 mirrors, 2 mirrors w/lens and 4 mirrors are included. (b) transmission loss in free space when using 45 degree coupler with/without lens and proximity coupler with lens from [5]

4. HIGH SPEED DATA COMMUNICATION

We also conducted high-speed test on the samples using the setup shown in Figure 4(a). Light from VCSEL is directly modulated at RF frequencies ranging from 1GHz to10GHz with random signal level of ±0.3V using Agilent ParBERT 81250 system. The separation between the input and the output boards is varied as before. The Q factors measured at d=0, d=1 mm and d=2 mm, with and without the inkjet-printed micro-lens, as shown in Figure 6(a). The corresponding Bit Error Rate (BER) data is shown in Figure 6(b). The Q factor decreased quickly for d=2 mm, indicating a high loss and large divergence of the beam in free space. In modern optical networks, data communication with a BER<10^{-9} is considered "error-free" [39, 40]. Without a micro-lens, at d=2 mm separation case, only data rate below 3 Gbps can be transmitted error-free. On the other hand, micro-lenses increase the error-free data transmission to 7 Gbps. It should be noted that using precisely positioned external lenses [26, 27] can help realize large separation coupling. However the results from Figure 6 show the integrated ink-jet printed micro-lens can be used as part of the proximity coupler for efficient transmission over short distances (<3mm).

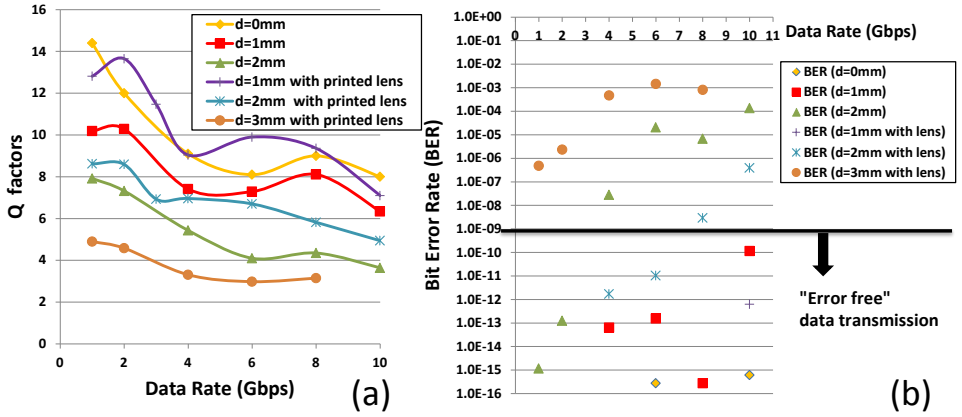

Figure 6 (a) Q factors with different data rate, at different separations. Two mirror couplers are included in optical path. (b) Bit Error Rate distribution (BER) with data rate at different separations with/without inkjet-printed lens.

5. CONCLUSIONS

We presented board-to-board optical interconnects using 45 degree mirror couplers and inkjet-printed micro-lens. The molding method using a low-cost electroplating technique was described and applied for optical layer fabrication. Micro-lenses (70 µm in diameter) were fabricated using an inkjet-printer. Each 45 degree mirror was shown to contribute about 1.88 dB loss (65% in coupling efficiency) to the total optical loss. The molded intra-board polymer

waveguides gave 0.18 dB/cm loss. When propagating in free space without a lens, 2 mm separation resulted 9.9 dB loss, which was reduced to 7.5 dB when a micro-lens was inserted in the path using inkjet printing. At this separation, the maximum error free data rate ($BER<10^{-9}$) was measured to be 3.5Gbps and 7.5Gbps, with and without the micro-lens, respectively. At 10Gbps with micro-lens presented, 1mm and 2mm separation yielded BERs of 6.2×10^{-13} and 3.9×10^{-7}, respectively. We expect that reducing the surface roughness and angle variation of the 45 degree mirror will further improve the coupling efficiency. Also printing micro-lenses on both the input 45 degree mirror and the PD or the receiving 45 degree mirror in a confocal setup will significantly reduce the free-space propagation loss. Furthermore, the profile control of ink-jet printed micro-lens needs to be optimized in order to further increase the coupling efficiency. To achieve an optimized lens profile, lens material properties and substrate surface energy should be carefully studied. To the best of our knowledge, this is the first report of free-space coupling between waveguides on separate boards.

Acknowledgements

This work was supported in part by the National Science Foundation. The fabrication and characterization facilities at MRC of the University of Texas are supported through NNIN program.

References

[1] L. Brusberg, M. Neitz, and H. Schroder, "Single-mode glass waveguide technology for optical inter-chip communication on board-level," Optoelectronic Interconnects Xii, 8267, (2012).

[2] J. Xue, A. Garg, B. Ciftcioglu *et al.*, "An Intra-Chip Free-Space Optical Interconnect," Isca 2010: The 37th Annual International Symposium on Computer Architecture, 94-105 (2010).

[3] R. T. Chen, L. Lin, C. Choi *et al.*, "Fully embedded board-level guided-wave optoelectronic interconnects," Proceedings of the Ieee, 88(6), 780-793 (2000).

[4] C. C. Choi, L. Lin, Y. J. Liu *et al.*, "Flexible optical waveguide film fabrications and optoelectronic devices integration for fully embedded board-level optical interconnects," Journal of Lightwave Technology, 22(9), 2168-2176 (2004).

[5] H. P. Kuo, P. Rosenberg, R. Walmsley *et al.*, "Free-space optical links for board-to-board interconnects," Applied Physics a-Materials Science & Processing, 95(4), 955-965 (2009).

[6] K. Nakama, Y. Matsuzawa, Y. Tokiwa *et al.*, "Board-to-Board Optical Plug-In Interconnection Using Optical Waveguide Plug and Micro Hole Array," Ieee Photonics Technology Letters, 23(24), 1881-1883 (2011).

[7] J. Van Erps, N. Hendrickx, C. Debaes *et al.*, "Discrete out-of-plane coupling components for printed circuit board-level optical interconnections," Ieee Photonics Technology Letters, 19(21-24), 1753-1755 (2007).

[8] J. J. Yang, A. S. Flores, and M. R. Wang, "Array waveguide evanescent ribbon coupler for card-to-backplane optical interconnects," Optics Letters, 32(1), 14-16 (2007).

[9] A. Flores, S. Y. Song, J. J. Yang *et al.*, "High-Speed Optical Interconnect Coupler Based on Soft Lithography Ribbons," Journal of Lightwave Technology, 26(13-16), 1956-1963 (2008).

[10] P. Pepeljugoski, and D. Kuchta, "Jitter Performance of Short Length Optical Interconnects for Rack-to-Rack Applications," Ofc: 2009 Conference on Optical Fiber Communication, Vols 1-5, 1797-1799 (2009).

[11] J. Sakai, A. Noda, M. Yamagishi *et al.*, "20Gbps/ch Optical Interconnection between SERDES Devices over Distances from Chip-to-Chip to Rack-to-Rack," 2008 34th European Conference on Optical Communication (Ecoc), (2008).

[12] J. W. Goodman, F. J. Leonberger, S. Y. Kung *et al.*, "Optical Interconnections for Vlsi Systems," Proceedings of the Ieee, 72(7), 850-866 (1984).

[13] D. A. B. Miller, "Optical interconnects to silicon," Ieee Journal of Selected Topics in Quantum Electronics, 6(6), 1312-1317 (2000).

[14] E. M. Strzelecka, D. A. Louderback, B. J. Thibeault *et al.*, "Parallel free-space optical interconnect based on arrays of vertical-cavity lasers and detectors with monolithic microlenses," Applied Optics, 37(14), 2811-2821 (1998).

[15] E. M. Strzelecka, G. D. Robinson, L. A. Coldren *et al.*, "Fabrication of refractive microlenses in semiconductors by mask shape transfer in reactive ion etching," Microelectronic Engineering, 35(1-4), 385-388 (1997).

[16] J. Chou, K. Yu, D. Horsley *et al.*, "Characterization of a MEMS Based Optical System for Free-Space Board-to-Board Optical Interconnects," 2010 Conference on Optical Fiber Communication Ofc Collocated National Fiber Optic Engineers Conference Ofc-Nfoec, (2010).

[17] F. Y. Wu, V. J. Logeeswaran, M. S. Islam *et al.*, "Integrated receiver architectures for board-to-board free-space optical interconnects," Applied Physics a-Materials Science & Processing, 95(4), 1079-1088 (2009).
[18] C. J. Henderson, B. Robertson, D. G. Leyva *et al.*, "Control of a free-space adaptive optical interconnect using a liquid-crystal spatial light modulator for beam steering," Optical Engineering, 44(7), (2005).
[19] J. H. Choi, L. Wang, H. Bi *et al.*, "Effects of thermal-via structures on thin-film VCSELs for fully embedded board-level optical interconnection system," Ieee Journal of Selected Topics in Quantum Electronics, 12(5), 1060-1065 (2006).
[20] L. Schares, J. A. Kash, F. E. Doany *et al.*, "Terabus: Terabit/second-class card-level optical interconnect technologies," Ieee Journal of Selected Topics in Quantum Electronics, 12(5), 1032-1044 (2006).
[21] C. T. Chen, H. L. Hsiao, C. C. Chang *et al.*, "4 channels x 10-Gbps optoelectronic transceiver based on silicon optical bench technology," Optoelectronic Interconnects Xii, 8267, (2012).
[22] B. Van Hoe, E. Bosman, J. Missinne *et al.*, "Novel coupling and packaging approaches for optical interconnects," Optoelectronic Interconnects Xii, 8267, (2012).
[23] J. Inoue, T. Ogura, K. Kintaka *et al.*, "Fabrication of Embedded 45-Degree Micromirror Using Liquid-Immersion Exposure for Single-Mode Optical Waveguides," Journal of Lightwave Technology, 30(11), 1563-1568 (2012).
[24] G. M. Jiang, S. Baig, and M. R. Wang, "Soft Lithography Fabricated Polymer Waveguides with 45 degrees Inclined Mirrors for Card-to-Backplane Optical Interconnects," Optoelectronic Interconnects Xii, 8267, (2012).
[25] A. L. Glebov, M. G. Lee, and K. Yokouchi, "Integration technologies for pluggable backplane optical interconnect systems," Optical Engineering, 46(1), (2007).
[26] B. Ciftcioglu, G. Jing, R. Berman *et al.*, "Recent progress on 3-D integrated intra-chip free-space optical interconnect." 56-57.
[27] B. Ciftcioglu, R. Berman, S. Wang *et al.*, "3-D integrated heterogeneous intra-chip free-space optical interconnect," Optics Express, 20(4), 4331-4345 (2012).
[28] X. L. Wang, W. Jiang, L. Wang *et al.*, "Fully embedded board-level optical interconnects from waveguide fabrication to device integration," Journal of Lightwave Technology, 26(1-4), 243-250 (2008).
[29] X. Y. Dou, X. L. Wang, H. Y. Huang *et al.*, "Polymeric waveguides with embedded micromirrors formed by Metallic Hard Mold," Optics Express, 18(1), 378-385 (2010).
[30] X. Lin, A. Hosseini, A. X. Wang *et al.*, "Reduced surface roughness with improved imprinting technique for polymer optical components." 280-281.
[31] R. Barbieri, P. Benabes, T. Bierhoff *et al.*, "Design and construction of the high-speed optoelectronic memory system demonstrator," Applied Optics, 47(19), 3500-3512 (2008).
[32] C. H. Tien, C. H. Hung, and T. H. Yu, "Microlens Arrays by Direct-Writing Inkjet Print for LCD Backlighting Applications," Journal of Display Technology, 5(4-6), 147-151 (2009).
[33] J. Y. Kim, N. B. Brauer, V. Fakhfouri *et al.*, "Hybrid polymer microlens arrays with high numerical apertures fabricated using simple ink-jet printing technique," Optical Materials Express, 1(2), 259-269 (2011).
[34] V. Fakhfouri, N. Cantale, G. Mermoud *et al.*, "Inkjet printing of SU-8 for polymer-based MEMS a case study for microlenses," Mems 2008: 21st Ieee International Conference on Micro Electro Mechanical Systems, Technical Digest, 407-410 (2008).
[35] J. P. Lu, W. K. Huang, and F. C. Chen, "Self-positioning microlens arrays prepared using ink-jet printing," Optical Engineering, 48(7), (2009).
[36] I. A. Grimaldi, A. D. Del Mauro, F. Loffredo *et al.*, "Microlens array manufactured by inkjet printing: study of the effects of the solvent and the polymer concentration on the microstructure shape," Optical Measurement Systems for Industrial Inspection Vii, 8082, (2011).
[37] A. Voigt, U. Ostrzinski, K. Pfeiffer *et al.*, "New inks for the direct drop-on-demand fabrication of polymer lenses," Microelectronic Engineering, 88(8), 2174-2179 (2011).
[38] K. H. Jeong, and L. P. Lee, "A new method of increasing numerical aperture of microlens for biophotonic MEMS," 2nd Annual International Ieee-Embs Special Topic Conference on Microtechnologies in Medicine & Biology, Proceedings, 380-383 (2002).
[39] F. Morichetti, A. Melloni, C. Ferrari *et al.*, "Error-free continuously-tunable delay at 10 Gbit/s in a reconfigurable on-chip delay-line," Optics Express, 16(12), 8395-8405 (2008).
[40] H. C. H. Mulvad, L. K. Oxenlowe, M. Galili *et al.*, "1.28 Tbit/s single-polarisation serial OOK optical data generation and demultiplexing," Electronics Letters, 45(5), 280-U60 (2009).